Chapter 3

High-throughput fractionation coupled to mass spectrometry for improved quantitation in metabolomics

Based on:

Tom van der Laan, Anne-Charlotte Dubbelman, Kevin Duisters, Alida Kindt, Amy C. Harms and Thomas Hankemeier

High-throughput fractionation coupled to mass spectrometry for improved quantitation in metabolomics

Analytical Chemistry (2020)

ABSTRACT

Metabolomics is emerging as an important field in life sciences. However, a weakness of current mass spectrometry (MS) based metabolomics platforms is the time-consuming analysis and the occurrence of severe matrix effects in complex mixtures. To overcome this problem, we have developed an automated and fast fractionation module coupled on-line to MS. The fractionation is realized by the implementation of three consecutive high performance solid-phase extraction columns consisting of a reversed phase, mixed-mode anion exchange and mixed-mode cation exchange sorbent chemistry. The different chemistries resulted in an efficient interaction with a wide range of metabolites based on polarity and charge and allocation of important matrix interferences like salts and phospholipids. The use of short columns and direct solvent switches allowed for fast screening (3 min per polarity). In total, 50 commonly-reported diagnostic or explorative biomarkers were validated with a limit of quantification that was comparable with conventional LC-MS(/MS). In comparison with a flow injection analysis without fractionation, ion suppression decreased from 89% to 25% and the sensitivity was 21 times higher. The validated method was used to investigate the effects of circadian rhythm and food intake on several metabolite classes. The significant diurnal changes that were observed stress the importance of standardized sampling times and fasting states when metabolite biomarkers are used. Our method demonstrates a fast approach for global profiling of the metabolome. This brings metabolomics one step closer to the implementation into the clinic.

INTRODUCTION

Metabolomics is increasingly important in the field of life sciences. It is used for the screening of inborn errors of metabolism[1], precision medicine[2] and discovery of new biomarkers for health, disease and intervention.[3] To accommodate this increased interest, there is a need for fast and comprehensive screening of the metabolome.[4] Mass spectrometry (MS) is a highly sensitive technique and MS-based methods can screen a large range of metabolites in a single run.[5] This makes MS highly suitable for comprehensive metabolomics. The downside of MS is that it often requires extensive sample preparation and separation to reduce interferences of complex biological samples at the ionization source.[6]

Flow injection analysis coupled to mass spectrometry (FIA-MS) is an appealing approach in fast and comprehensive screening since there is no chromatography that discriminates against compound classes or decreases the throughput.[7] The sample preparation of these methodologies is often a 'dilute-and-shoot' approach, whereby dilution is applied to decrease the interference of the sample matrix at the ionization source. However, these methods often suffer in terms of sensitivity because the analytes are also diluted or high abundant matrix interferences still cause severe ion suppression.[8] Therefore, sample preparation remains an important aspect in fast MS analysis in order to decrease the sample complexity while maintaining a sufficient analyte concentration. Liquid-liquid extraction (LLE) has been performed in parallel and coupled to FIA-MS to improve throughput and coverage.[9] On the other hand, solid-phase extraction (SPE) has been coupled on-line to mass spectrometry in the RapidFire system resulting in analyses times of around 8.5 seconds.[10] By using LLE or different SPE sorbents in parallel, however, the cleanup efficiency remains limited. Generally, these approaches only result in two fractions (water/organic fraction in LLE and flow-through/elution fraction in SPE) and fractions are ionized at once without within-fraction separation.

In this work, we demonstrate a comprehensive and fast sample preparation method coupled on-line to MS. The method utilizes two important chemical properties of the metabolome: polarity and charge. Three consecutive high performance (particle size ≤5 µm) SPE columns, consisting of a reversed phase, mixed-mode cation exchange and mixed-mode anion exchange sorbent chemistry, are coupled on-line to a mass spectrometer. This ensured the allocation of metabolites into different fractions (flow-through; polar/neutral, reversed phase; apolar, cation exchange; polar and positive, anion exchange; polar and negative). Moreover, it also removed known ion suppressors from different fractions minimizing their adverse effects during electrospray ionization. Phospholipids and salts are held responsible for a majority of signal suppression during electrospray ionization of plasma samples.[11] By using a fractionation approach based on polarity and charge, phospholipids are retained on the reversed phase column whereas positive

and negative salt ions are trapped on and eluted from the cation and anion exchange, respectively. Another benefit of serially coupled columns is the flow-through fraction, which is cleaned by three sorbent chemistries instead of one in conventional single-column methods. The advantage of on-line fractionation over off-line fractionation is that it allows for some separation between compounds within a fraction prior to electrospray ionization. Hereby, retained ion suppressors could elute at another time than retained analytes. To our knowledge, this is the first publication that reports the use of serially coupled high performance SPE columns to realize an on-line fractionation including some separation prior to MS analysis. The strength of this platform is emphasized by the use of short analytical columns which allow for fast solvent switches while still benefitting from chromatographic separation.

We have developed a targeted platform for the analysis of 50 commonly-reported diagnostic or explorative biomarkers.[12,13,14] These compounds belong to the following compound classes: amino acids, amines, purines, sugars, acylcarnitines, organic acids and fatty acids. We present a fast on-line sample preparation method that fractionates these compound classes in plasma. Several on-line SPE columns have been evaluated for their ability to fractionate plasma prior to MS analysis. The optimized methods for both positive and negative electrospray ionization mode have been validated and applied in a study investigating the effect of circadian rhythm and food intake on several metabolite classes. This study should give insight into the diurnal variations of the studied biomarkers. These variations are important to assess because they could potentially be misinterpreted as disease or intervention related variations. This misinterpretation compromises the diagnostic and explorative power of a potential biomarker.

MATERIALS & METHODS

Chemicals

An overview of the used (internal) standards and concentrations is provided in the Supplementary information (Table S1 and S2). Water was obtained from an arium pro UF/VF water purification system with a Sartopore 2 0.2 µm filter. Methanol (Ultra-LC-MS grade) was purchased from Actu-All (Oss, The Netherlands). Ammonium hydroxide (28-30 wt% solution of ammonia in water) and formic acid (98%+) were purchased from Acros Organics (Bleiswijk, The Netherlands). Ammonium acetate (≥99.0%) and ammonium formate (≥99.995%) were purchased from Sigma-Aldrich (Zwijndrecht, The Netherlands).

Method development

We have used polymeric mixed-mode ion exchange columns because they provide a superior pH stability over other ion exchange sorbent types. Several ion exchange columns have been evaluated according to the retention, trapping and elution performances of representative

standards. We tested four low performance (particle size >5µm), four high performance Sepax (particle size 1.7-5µm) and four high performance Zirchrom (particle size 3µm) SPE columns. The low performance, Sepax and Zirchrom SPE columns were composed of four mixed-mode ion exchange types (strong cation exchange (SCX), strong anion exchange (SAX), weak cation exchange (WCX) and weak anion exchange (WAX)). Similar loading and elution buffers were used for each type of ion exchange. The evaluated ion exchange columns, loading and elution buffers explored during development can be found in the Supplementary information (Table S3). The selected ion exchange columns were coupled to a reversed phase column and ordered in a way that was most beneficial in terms of matrix effect reduction and peak shape. The reversed phase column was a ZORBAX Extend-C18, 2.1 mm × 5 mm, 1.8 µm guard column from Agilent Technologies Netherlands (Waldbronn, The Netherlands).

Five cationic compounds were used to represent different types of cations (leucine, glutamic acid, arginine, hypoxanthine and choline) and four anionic compounds were used to represent different types of anions (lactic acid, malic acid, citric acid and indoxyl sulfate). The amino acids consisted of cationic and anionic functional groups. Glucose functioned as a neutral marker and indicated whether ions were efficiently removed from the column flow-through.

Validation

Individual stock solutions and calibration mixtures were stored at -80 ˚C. In each specific fraction, there was at least one internal standard present. In total seven calibration points were used (C1-7). The highest calibration concentration is referred to as C7 (Supplementary information Table S1) and the subsequent concentrations were 1:1 dilutions of the previous concentration. All calibration standards were included in the same stock solution and all calibration solutions were composed of 69% methanol in water. C0 was prepared by adding 69% MeOH without standards. Within the calibration range, C4 and the internal standard concentration were set to mimic the physiological concentration of the analyte found on the Human Metabolome Database (HMDB).[15] Calibration curves were constructed by standard addition of the calibration standards to plasma samples. The repeatability of the method was determined by the relative standard deviation of three replicates of three different concentrations (C0, C2 and C4). The intermediate precision was determined by the relative standard deviation of three different concentrations (C0, C2 and C4) on three different days (N=9). The matrix effect was determined by the ratio of the peak area of the internal standard in a plasma and water sample.[16] Ion suppression was determined by subtracting 100% by the matrix effect. Ion suppression of ion enhanced compounds was set at 0% when calculating the mean ion suppression.

$$(1)\ Matrix\ effect = \frac{Area\ ISTD\ in\ plasma}{Area\ ISTD\ in\ water} \times 100\%$$

$$(2)\ Ion\ suppression = 100\% - Matrix\ effect$$

The carryover was evaluated as the ratio of the peak area in a blank sample and the peak area in a pooled plasma sample that was analyzed just before the blank (N=3). Ten concentration levels of internal standards were used to determine the limit of detection (LOD) and lower limit of quantification (LLOQ). The highest concentration was C6 which was four times the physiological value of the unlabeled counterpart (Supplementary information Table S2) and the subsequent concentrations were 1:1 dilutions of the previous concentration. The LOD (formula 3) and LLOQ (formula 4) were determined by the following formula which used the peak area of a blank, the standard deviation (SD) of the lowest concentration with a S/N greater than 3 (C_{low}) and the response factor (RF), which was calculated by the ratio of the peak area and concentration of C_{low}.

$$(3)\ LOD = \frac{3 \times SD_{area\ Clow} + area_{Blank}}{\left(\frac{area_{C_{low}}}{[C_{low}]}\right)}$$

$$(4)\ LLOQ = \frac{10 \times SD_{area\ C_{low}} + area_{Blank}}{\left(\frac{area_{C_{low}}}{[C_{low}]}\right)}$$

Sample preparation

During the method validation, 30 µL EDTA plasma aliquots, 30 µL of calibration standard and 30 µL of the internal standard solution, H_2O and MeOH were mixed reaching a total volume of 195 µL and 71% MeOH. The mixture was vigorously vortexed and centrifuged (10 min, 16100 g, 4 °C). After centrifugation, 100 µL of the supernatant was transferred into an autosampler vial containing a 150 µL insert. Study samples were prepared by mixing 15 µL EDTA, 15 µL of internal standard solution, H_2O and MeOH reaching a total volume of 97.5 µL and 71% MeOH (same ratios as during method validation). The vortex and centrifuge step remained the same and 50 µL of the supernatant was transferred into an autosampler vial containing a 150 µL insert.

The flow injection analysis (FIA) sample preparation was adapted from Carducci *et al.*[17] Ten microliters of EDTA plasma and internal standard solution were mixed with methanol, water and acetic acid to reach a final solution of 80% methanol, 0.1% acetic acid and a plasma dilution ratio of 100. This dilution ratio was found to give the highest sensitivity after testing plasma dilution ratios of 10 to 500. An adjusted Bligh and Dyer LLE was also performed prior to the FIA.[18] Ten microliters of EDTA plasma and internal standard solution were extracted with methanol, dichloromethane and water (v/v/v, 2/2/1.8) reaching a total volume of 1000 µL. 200 µL of the

apolar and 200 µL of the polar fraction were evaporated and separately reconstituted in 200 µL 0.1% acetic acid in 80% MeOH.

Fractionation and mass spectrometry

A Shimadzu Nexera UHPLC (Darmstadt, Germany) was connected to a Sciex X500R QToF (Darmstadt, Germany). The setup was extended by a stand-alone Agilent 1260 Infinity Isocratic Pump (Waldbronn, Germany) and two VICI six-port valves (Rotterdam, The Netherlands). Figure 1 shows a schematic overview of the setup.

The injection volume of the fractionation method was set at 1 µL and the flow rate at 800 µL/min. In positive mode, the C18, WAX and SCX columns were loaded consecutively. The mobile phases consisted of 0.2% formic acid in water for loading (gradient pump: A), 2 mM ammonium acetate in methanol for the C18 elution (gradient pump: B) and 100 mM ammonium acetate pH 10 for ion exchange elution (IEX pump). In negative mode, the C18 and WAX columns were loaded consecutively. The mobile phases consisted of 2 mM ammonium acetate in water for loading (gradient pump: A), 2 mM ammonium acetate in methanol (gradient pump: B) for the C18 elution and 100 mM ammonium formate pH 10.5 for ion exchange elution (IEX pump). When the gradient pump was selected, the IEX pump pumped the solvent back to the solvent bottle. When the IEX pump was selected, the gradient pump flow was directed to waste. By using two other six-port valves, the IEX columns could be switched in and out of the line of the LC flow. The total runtime

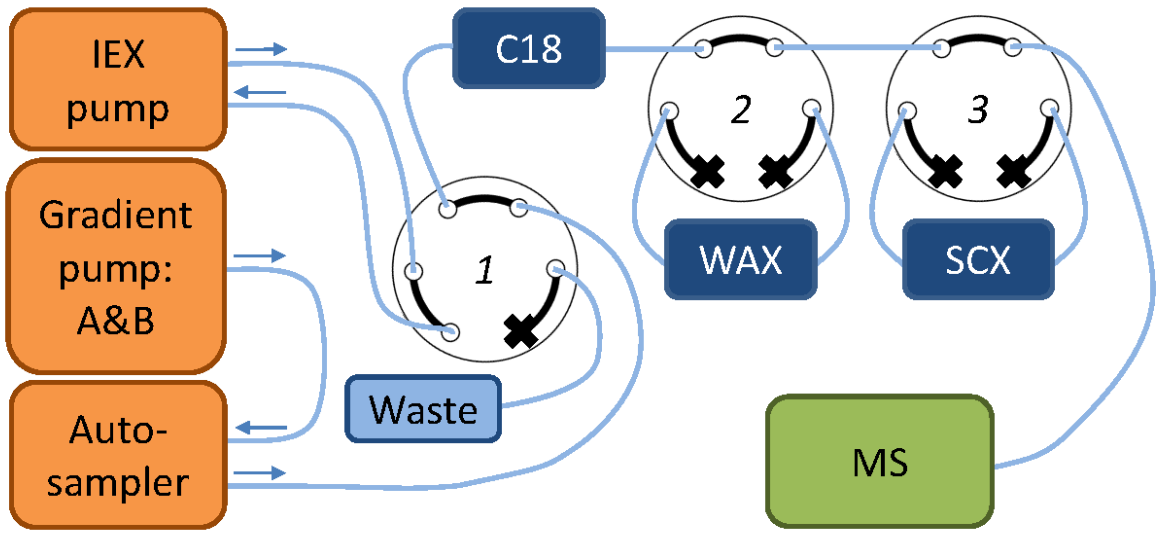

Figure 1. Schematic representation of the on-line fractionation setup. Valve 1, which was located on the mass spectrometer, was used to change between the IEX pump and the gradient pump. Valve 2 and 3, VICI valves, were used to switch the ion exchange columns in or out of line.

was 3 min and the detailed timetable of the fractionation in positive and negative mode can be found in the Supplementary information (Table S4 and S5).

The flow injection analysis (FIA) method was adapted from Carducci *et al.*[17] The injection volume was set at 20 µL and the flow rate at 80 µL/min. The mobile phase consisted of 80% methanol in water. Although the mobile phase contained no additives, the sample diluent contained 0.1% acetic acid which was suf-ficient to promote ionization. At 0.8 minutes, the flow rate was increased to 800 µL/min for 0.5 minutes in order to flush the system and at 1.3 minutes the flow rate returned to 80 µL/min. The total analysis time was 1.4 minutes. The MS parameters can be found in the Supplementary information (Table S6).

The data was processed in Analytics of Sciex OS 1.6. For the targeted processing, the analytes were integrated by integrating the signal of the M+H (in positive mode) and M-H (in negative mode) ion with an XIC width of 0.01 Dalton. Glucose was measured as an M+Na ion and choline was measured as an M+ ion. The untargeted data processing was performed using the 'Non-targeted Peaks' function in Analytics (see detailed information in the Supplementary information table S11C).

Effect of circadian rhythm and food intake on metabolite classes

The effect of circadian rhythm and food intake on the metabolite classes was evaluated for ten healthy male volunteers (aged 18-45 years). The clinical study was approved by the Ethical Committee of the Centre for Human Drug Research Leiden and all volunteers signed an informed consent form. The study design has previously been published.[19] In short, blood samples were collected over 24 hours under uniform conditions for food intake, physical activity and night rest. At each time point, 20 mL of blood was drawn into two 10 mL BD Vacutainer® K2EDTA tubes and kept on ice. The tubes were gently inverted multiple times and centrifuged (1000 g, 15 min, 4 °C). Plasma samples were aliquoted and stored at -80 ˚C prior to analysis. A quality control (QC) was prepared by pooling 15 µL of every individual study sample. A QC sample was analyzed every 10 samples. Metabolites with an RSD below 15% throughout the QC samples were included in the data analysis.

Each metabolite was normalized on the first time point and subsequently log-transformed using the natural logarithm. Then, the metabolites were allocated to six different compound classes (amino acids, amines, hexose, acylcarnitines, organic acids or fatty acids). An overview of the compound classes is provided in the Supplementary information (Table S7). Within each compound class, all metabolite concentrations were averaged per time point and volunteer. A Wilcoxon Signed Rank test was used to assess the change in this mean per time point relative to

the baseline.[20] A multiple comparisons correction (Benjamini–Yekutieli, < 0.1) was used to adjust the p-values for multiple testing.[21] All statistical analyses were performed in R (version 3.4.3).[22]

RESULTS AND DISCUSSION

Method development

This study aims to develop an efficient and fast methodology to minimize matrix effects, focusing on salt and (phospho)lipid removal. Lipid removal was accomplished by a reversed phase column and salt removal by mixed-mode ion exchange columns. An Agilent ZORBAX Extend-C18 UPLC guard column was selected as the reversed phase column because it demonstrated superior separation and peak shape over low performance SPE columns.

Table 1 provides an overview of the performance of the evaluated ion exchangers. The grading scheme is depicted by numbers and colours indicating good (positive and green) or bad (negative and red) performances. Table 1 indicates that the WCX columns had a relatively low trapping efficiency as most of the analytes eluted at the dead time (grade 0). Most of the analytes were efficiently retained or trapped (grades 1 and 2, respectively) by the SCX columns. However, choline could not be eluted in the Hysphere column and arginine caused breakthrough (grade -1) in the Zirchrom column indicating a superior performance of the Sepax column. The right part of Table 1 shows that all SAX columns did not allow the desorption of indoxyl sulfate (grade -3) indicating that this type of anion exchanger could be exhausted over time due to the irreversible

Table 1. Evaluation of different mixed-mode cation and anion exchange columns. The grading scheme is as follows: elution at dead time: 0; retention: 1; trapped and eluted: 2; trapped and separated during elution: 3; no peak visible: -3; extreme tailing: -2; breakthrough: -1).

		Low performance		High performance			
		Hysphere	Oasis	Sepax		Zirchrom	
		Strong	Weak	Strong	Weak	Strong	Weak
Cation exchange	Leu	2	0	1	0	0	1
	Glu	2	0	1	0	2	-2
	Arg	-2	1	2	0	-1	2
	Hpx	2	0	1	0	0	0
	Choline	-3	-2	1	0	0	1
Score		1	-1	6	0	1	2
Anion exchange	Lactate	-1	1	1	1	-3	-2
	Malate	2	2	2	2	-3	-2
	Citrate	2	2	-2	2	-3	-2
	Indoxyl sulfate	-3	-3	-3	3	-3	2
Score		0	2	-2	8	-12	-4

binding of analytes. The Sepax WAX was suitable for all representative analytes, whereas the Oasis column was too strong (grade -3 for indoxyl sulfate) and the Zirchrom column repeatedly resulted in extreme tailing (grade -2). The Sepax SCX and WAX columns were unsurpassed in terms of retention and trapping and allowed for the analysis of all representative compounds. Therefore, we selected these columns for the trapping of the ionic species. The combination of a WAX and SCX also provided the possibility to use a similar elution buffer for both columns. The elution from a WAX column requires a high pH in order to remove the positive charge on the sorbent, whereas the high pH removes the positive charge of the analytes during the elution of an SCX column. Besides, the high pH is accomplished by the use of ammonia, which is a suitable counter-ion for an SCX column.

The silica material of the ZORBAX Extend-C18 guard column was end-capped with methyl groups which made the sorbent resistant to high pH. Therefore, this particular column could be permanently in line with the flow. In contrast, the IEX columns were switched out of the line during C18 elution because this improved retention. In negative mode, the WAX elution profile was better in the absence of the SCX column. Since the SCX column did not contribute to the reduction of ion suppression in negative mode, this column was permanently switched out of the line during the analysis in negative mode. The IEX methods were further optimized to improve retention and peak shapes and to minimize carry-over.

Fractionation characteristics

Figure 2 shows the chromatograms of a pooled plasma sample measured with the final fractionation methods in positive and negative mode. The chromatogram contains three different fractions in positive mode (flow-through: polar neutral/positive; IEX: polar positive and C18: apolar) and three fractions in negative mode (flow-through: polar neutral/negative; IEX: polar negative and C18: apolar). An overview of the fractions and charge of the analytes during loading is supplied in the Supplementary information (Table S7). The elution profile of the phospholipids in the negative fractionation method is measured in positive MS polarity (because of ionization efficiency) and shown in the Supplementary information (Figure S1). The phospholipids are separated from both the acylcarnitines and the fatty acids and therefore could not suppress their ionization. This stresses the importance of the combined on-line fractionation and separation. If these fractions were collected off-line and subsequently injected into the MS, the phospholipids would have been ionized simultaneously with the fatty acids and acylcarnitines. The salts were most likely divided over the mixed-mode ion exchangers (SCX and WAX in positive mode and WAX in negative mode) and eluted during the ion exchange elution. By allocating these known ion suppressors over different fractions, we minimized the ion suppression in a limited amount of time.

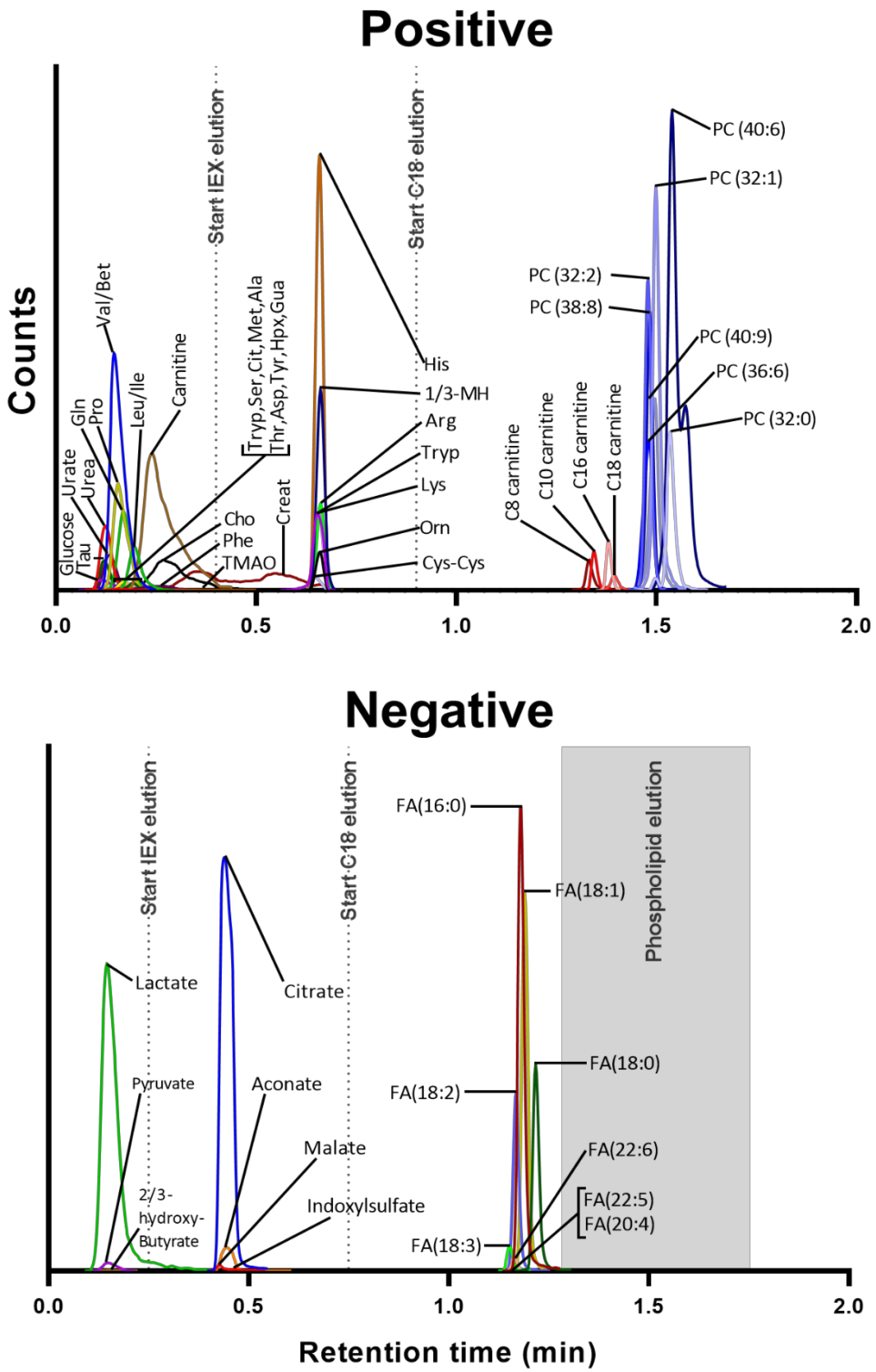

Figure 2. Extracted ion chromatogram of a pooled plasma sample measured by the fractionation method in positive and negative mode. The phospholipid elution window (phospholipid elution profile shown in Supplementary information Figure S1) in negative mode is indicated by the grey area. All the ions are measured by M+H in positive mode and M-H in negative mode, apart from hexose which was measured as a sodium adduct. For visualization purposes, the phospholipids and fatty acids were extracted by using the one 13C m/z value.

In general, the flow-through fraction contained analytes that were polar and consisted of a zero and/or one net charge during loading. Singly-charged compounds experienced some retention in positive mode, but no retention in negative mode. The lack of retention might be explained by the counter-ion effect of the high concentrations of salts in plasma. In positive mode, a remaining negative charge on the acids might have impaired the retention of amino acids. The second fraction comprised all the components that were trapped on the ion exchange columns. A compound was efficiently trapped on the IEX column if it consisted of multiple net charges or was in equilibrium between one net charge and multiple charges at the pH during loading. The third fraction consisted of all the apolar compounds, which were efficiently trapped on and eluted from the C18 column.

Creatinine was strongly retained but not trapped on the SCX column. Creatinine had one positive net charge and two additional neutral nitrogen atoms, which could have potentially increased the interaction with the stationary phase. We did not find any other compounds that resulted in multiple peaks due to breakthrough or multiple trappings. Non-gaussian shaped peak areas were obtained by integrating the area under the curve between the two intersections with the baseline. These compounds were corrected by their corresponding internal standard because their peak shape and retention time were similar (see Supplementary information Figure S2 for the example of creatinine(-D3)). Other analytes were corrected either by their corresponding internal standard or by an internal standard that coeluted. the area under the curve between the two intersections with the baseline. These compounds were corrected by their corresponding internal standard because their peak shape and retention time were similar (see Supplementary information Figure S2 for the example of creatinine(-D3)). Other analytes were corrected either by their corresponding internal standard or by an internal standard that coeluted.

Method validation

The validation was performed by assessing the repeatability, intermediate precision, carryover, LOD, LLOQ and the matrix effect of the method. The results of the validation can be found in Supplementary information (Table S8).

The mean repeatability and intermediate precision were 6.0 and 7.1%, respectively. The relative standard deviation of 48 compounds was below 15% and two components varied more than 15%: TMAO and guanine. This was most likely caused by the low signal of these analytes due to the low physiological concentration and the low molecular weight. In total, 1071 injections were performed on the same set of columns with a sufficient repeatability as is shown in the validation (first injections) and biological application (last injections). The coefficient of determination (R^2) was on average 0.995, which indicated a good linearity of the fractionation method. The linearity of 47 compounds was higher than 0.99 and three compounds revealed a linearity lower than 0.99.

The linearity of C16- and C18-carnitine was compromised by matrix interferences since a calibration curve constructed in water demonstrated a sufficient linearity (>0.99). All the acylcarnitines were corrected by the same internal standard, i.e. octanoylcarnitine-d3. This internal standard corrected well for co-eluting analytes C8- and C10-carnitine. C16- and C18-carnitine were more strongly retained and eluted further away from the internal standard and closer to the (phospho)lipids. Therefore, the linearity of these analytes would be improved by the correction of a more apolar internal standard. The lower linearity of docosapentanoic acid was found for both plasma and water samples. The reason for this was unknown.

The LOD and LLOQ were determined by spiking several internal standards in plasma. This was done because the analytes of interest were endogenous and differences in chromatography were observed between water and plasma samples. Figure 3 demonstrates that physiological blood levels as reported in literature were higher than the calculated LLOQ indicating a sufficient sensitivity of the method. The average carryover was 0.5% when a blank sample was measured after a QC sample. In total 48 compounds demonstrated a lower carryover than 2%. There were two compounds with a higher carryover: methionine (5.3%) and decanoylcarnitine (2.4%). The carryover of methionine can be explained by the fact that sulfur sticks to stainless steel.[23] The reason for the carryover of decanoylcarnitine was unclear. Although a slight carryover has been observed, we expect no problems with respect to the quantification of study samples. The analytes of interest are endogenous compounds, which are present in every studied person. This will ensure that a small carryover will have a limited effect on the quantification values of the analytes.

Fractionation versus flow injection analysis and conventional liquid chromatography

In order to demonstrate the cleanup efficiency of the fractionation method, we measured spiked internal standards in plasma and water. Hereby, the matrix effect, ion suppression and LLOQ were determined for the fractionation and an FIA method. Figure 3 shows that the mean ion suppression of the fractionation method was 25%, whereas the mean ion suppression in the FIA method was 89%. We have previously reported the effects of salts and phospholipids on the ESI.[11] The fractionation method provides a fast solution to minimize ion suppression caused by these matrix interferences. The use of three orthogonal columns allocated phospholipids, negative and positive salts into three different fractions. The on-line elution into the MS and the use of high performance SPE columns allowed for the separation between analytes and matrix interferences within a fraction. An additional LLE step prior to the FIA decreased the ion suppression to 80% (see Supplementary information Table S9). This decrease in ion suppression was predominantly observed for compounds in the apolar fraction, i.e. fatty acids and acylcarnitines. However, the ion suppression of these compounds was still considerably less in our fractionation method. For

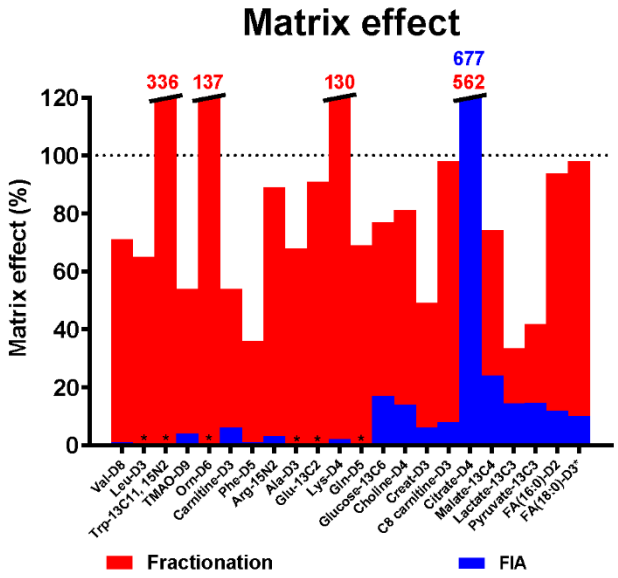

Internal standards	LLOQ (µM) FIA	LLOQ (µM) Frac	Physiological level (µM)
Val-D8	176	1	212
Leu-D3	171	2	61
Trp-13C11, 15N2	90	1	55
TMAO-D9	44	1	38
Orn-D6	240	10	67
Carnitine-D3	2	0.03	46
Phe-D5	82	4	78
Arg-15N2	11	0.5	114
Ala-D3	**	27	427
Glu-13C2	**	1	97
Lys-D4	22	4	179
Gln-D5	1345	4	510
Glucose-13C6	26	10	4971
Choline-D4	2	0.1	15
Creat-D3	18	0.3	87
C8 carnitine-D3	0.3	0.003	0.2
Citrate-D4	6	1	114
Malate-13C4	2	0.9	3.2
Lactate-13C3	71	13	1489
Pyruvate-13C3	24	19	35
FA(16:0)-D2	1.3	0.7	122
FA(18:0)-D3	0.6	0.6	49

*Figure 3: Performance comparison of the fractionation (Frac) method and flow injection analysis (FIA). The graph shows the matrix effect for each internal standard measured by either the fractionation method (red) or FIA (blue). Compounds with 0% matrix effect (indicated by *) were not detected at C4 levels. Compounds that experienced ion enhancement (matrix effect>100%) were cut off at a matrix effect of 120% (values are indicated in corresponding colours). The table on the right shows the lower limit of quantification (LLOQ) of FIA and fractionation as well as the physiological plasma levels (HMDB values).*[29] *(**=not detected at C7 levels)*

metabolites in the polar fraction, the ion suppression was comparable with FIA without LLE. LLE demonstrates little cleanup efficiency because samples are only fractionated based on polarity and the obtained fractions are analyzed at once without further separation.

The fractionation method demonstrated a superior sensitivity in comparison with FIA. The mean LLOQ of the fractionation method was 21 times lower which ensured a sufficient sensitivity to measure physiological levels in plasma. In contrast, 9 out of 22 analytes could not be quantified using the FIA method due to insufficient sensitivity (LLOQ higher than physiological levels). The substantial difference in ion suppression was most likely responsible for the differences in sensitivity. The performance improvement was mainly reflected in positive mode. In negative mode, the improvement in ion suppression and sensitivity was smaller. This is in accordance to other studies, in which was shown that ion suppression is less occurring in negative ionization mode.[24,25] Although the FIA method is faster (1.4 versus 3 min), the findings in Figure 3 emphasize the necessity of on-line fractionation prior to electrospray ionization.

We have also compared the LLOQ of the ISTDs with the LLOQ of conventional LC-MS analyses reported in literature (see Supplementary information Table S10). These findings demonstrated

that the sensitivity of fractionation and LC-MS is in a similar range. This was also expected because of the limited ion suppression in the fractionation method and a comparable peak width, injection volume and flow rate with regards to general LC-MS. However, differences in, for example, LLOQ determinations, used mass spectrometer (tandem and high-resolution) and derivatization might complicate this comparison. It does indicate that we are at least in a comparable sensitivity range relative to LC-MS. This is also emphasized by the coverage of the fractionation method in comparison with conventional reversed phase (RP) and hydrophilic interaction chromatography (HILIC) separations. The number of unique retention time and *m/z* features was 2289, 3475 and 3529 for fractionation, RP and HILIC, respectively (the methodologies are presented in the Supplementary information Table S11). The difference in coverage is mostly explained by the additional isomeric separation that is experienced in conventional chromatography as the number of unique *m/z* features was practically similar (2089, 2465 and 2325 for fractionation, RP and HILIC, respectively).

Our fractionation approach enables the analysis of multiple compound classes in 3 minutes per polarity, whereas conventional LC-MS usually requires a gradient time of around 3-30 minutes per compound class (see Table S10). The analysis time of LC-MS can be reduced by the use of faster gradients. However, in order to realize a comprehensive targeting of the metabolome, multiple LC separations would be needed (e.g. HILIC and RP for polar and apolar, respectively). The inclusion of multiple chromatographic gradients drastically decreases the overall throughput of the analysis. Moreover, the equilibration and flushing time of conventional LC columns (3-15 cm) is substantially higher in comparison with short chromatographic columns (0.5-1 cm). The benefit of an integrated fractionation approach is due to the use of multiple short chromatographic columns, which allow for an efficient separation, while little time is spent on gradients and column equilibration/flushing. The challenge of using a fractionation approach instead of conventional chromatography is the lack of isomeric separation. This could be overcome by the use of ion-mobility and MS/MS experiments.

Effect of circadian rhythm and food intake on metabolite classes

It is known that there are trends in metabolite levels due to the circadian rhythm and food intake.[26] These fluctuations are important to take into account when metabolites are studied or used as biomarkers. Different sampling times throughout the day could cause variations in metabolite levels that are not attributable to a studied disease or intervention. For this, we profiled ten healthy volunteers on ten different time points on a time scale of 24 hours. This study should clarify the significance of these diurnal changes.

After the data acquisition, 47 compounds were included in the data analysis and three compounds were excluded. Fatty acid 16:0 and 18:0 had an RSD of more than 15% due to fluctuating background levels. C18 carnitine also had an RSD of more than 15%. The reason for this was unclear. Figure 4 shows that our validated platform allowed us to demonstrate significant changes of metabolite classes throughout the day (false discovery rate (FDR) adjusted p-values are listed in the Supplementary information Table S12). All compound classes changed significantly from the baseline, apart from the amines. The amines (quaternary amines, creatinine, urea and uric acid) did not reveal a significant difference over a period of 24 hours. This is in accordance with our prior work, in which we demonstrated that gut metabolites (quaternary amines) were not affected by the fasting state of an individual.[11] The amino acid levels started to rise after wake time. The levels remained high throughout the morning/afternoon and decreased again towards baseline levels just before dinner. After dinner, the amino acids increased again and subsequently returned to baseline levels during night rest. The increase in amino acids after wake time and in the afternoon/evening has also been observed in prior studies.[20]

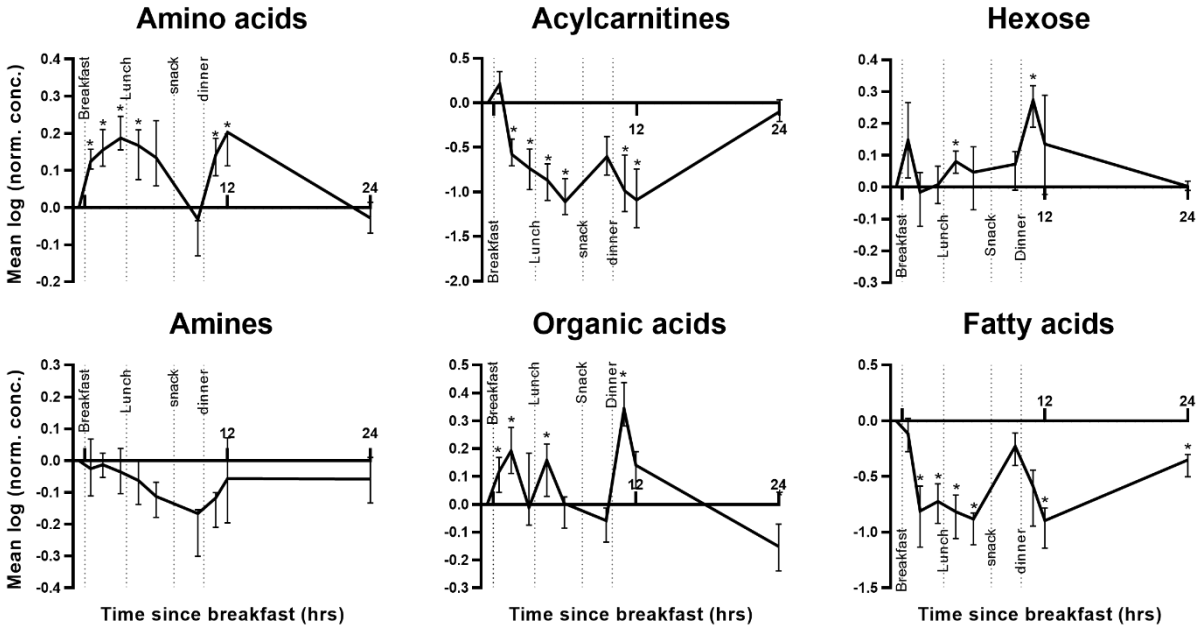

Figure 4. The mean natural logarithm of normalized metabolite concentrations over time. Within each compound class, metabolites were averaged per time point and volunteer. The mean of these curves over the 10 volunteers are depicted and the pointwise interquartile range (IQR) of the volunteers is presented in the error bars. Time points that are significantly different from the baseline are indicated (FDR adjusted p-values < 0.1). The time frame comprises four standardized feeding times and meals and one night rest. The time is presented with respect to the breakfast time.*

The hexose and organic acid levels significantly increased after the feeding times (except for hexose after breakfast which did not reach FDR corrected significance). When sugar is available, glucose is the main source of the citric acid cycle. This explains the similarities of the hexose and organic acid trends since organic acids are the main constituents in the citric acid cycle. The fatty acids concentrations decreased throughout the day and increased just before dinner and after 24 h, which has been observed before.[26] During (overnight) fasting, glucose is mainly depleted, switching the main energy source to fatty acids. In this state, fatty acids are released from triglycerides by lipolysis, which explains the high fatty acid levels prior to dinner and after a night rest.[27] In order to accommodate the increased demand for fatty acids, acylcarnitines are put in place to transport the fatty acids into the mitochondria for β-oxidation.[28] This explains the similarities between the fatty acid and acylcarnitine profile. Sampling time is an indispensable parameter to take into account when metabolites are used or studied as biomarkers. Food intake and circadian rhythm significantly change compound classes from baseline levels. Therefore, sampling times and fasting states should be standardized when metabolites are used for diagnosis, clinical studies or biomarker discovery. This should further strengthen the use of discovered metabolite biomarkers in personalized health care.

CONCLUSIONS

Although much progress has been made in the analysis of metabolites, fast and global profiling of the metabolome in complex matrices remains a challenging aspect. For this purpose, we demonstrated a fast and comprehensive fractionation method coupled on-line to mass spectrometry. The three serially coupled high performance SPE columns resulted in a fractionation based on polarity, charge, and removed important ion suppressors from different fractions. The on-line and orthogonal setup realized a flow-through which was cleaned by three different sorbent chemistries and a within-fraction separation of analytes and ion suppressors. The comparison with FIA emphasized the performance improvement achieved with the fractionation method. In a limited amount of time, the fractionation method drastically lowered the ion suppression as well as the detection limits. The on-line fractionation demonstrated similar quantification limits in comparison to the conventional LC-MS analyses. This proves that on-line fractionation enables the analysis of a large range of metabolites without suffering in terms of sensitivity. The developed fractionation method was able to demonstrate fluctuations of metabolite classes in blood samples from healthy volunteers on different time points throughout the day, which could be explained by underlying metabolic processes. These significant diurnal variations are important for clinicians when metabolites are used as biomarkers. Standardized sampling times and fasting states should minimize variations caused by food intake and circadian rhythm on the disease or intervention related variations. This work provides a methodology to

target multiple metabolite classes within a single analytical platform without suffering in terms of analysis time. This development in comprehensive and fast metabolite screening should encourage researchers and clinicians to make full use of the field of metabolomics and to further investigate the value of potential prognostic and diagnostic biomarker metabolites.

ACKNOWLEDGEMENTS

The authors are grateful to receive funding for this research from The Netherlands Organization for Scientific Research (NWO) in the framework of the Technology Area TA-COAST (Fund New Chemical Innovations. project no. 053.21.118). This research was also part of the Netherlands X-omics Initiative and partially funded by NWO, project 184.034.019.

REFERENCES

1. Mussap, M., Zaffanello, M. & Fanos, V. Metabolomics: a challenge for detecting and monitoring inborn errors of metabolism. **6**, (2018).
2. Balashova, E., Maslov, D. & Lokhov, P. A Metabolomics Approach to Pharmacotherapy Personalization. *J. Pers. Med.* **8**, 28 (2018).
3. Kaushik, A. K. & DeBerardinis, R. J. Applications of metabolomics to study cancer metabolism. *Biochim. Biophys. Acta - Rev. Cancer* **1870**, 2–14 (2018).
4. Miggiels, P., Wouters, B., Westen, G. J. Van, Dubbelman, A. & Hankemeier, T. Novel technologies for metabolomics: more for less. *TrAC - Trends Anal. Chem.* **2018**, 1–9 (2018).
5. Gowda, G. A. N. & Djukovic, D. Overview of Mass Spectrometry-Based Metabolomics: Opportunities and Challenges. *Methods Mol Biol* **1198**, 3–12 (2014).
6. Ismaiel, O. A., Halquist, M. S., Elmamly, M. Y., Shalaby, A. & Karnes, H. T. Monitoring phospholipids for assessment of matrix effects in a liquid chromatography-tandem mass spectrometry method for hydrocodone and pseudoephedrine in human plasma. *J. Chromatogr. B Anal. Technol. Biomed. Life Sci.* **859**, 84–93 (2007).
7. Enot, D. P. *et al.* Preprocessing, classification modeling and feature selection using flow injection electrospray mass spectrometry metabolite fingerprint data. *Nat. Protoc.* **3**, 446–470 (2008).
8. Nanita, S. C. & Kaldon, L. G. Emerging flow injection mass spectrometry methods for high-throughput quantitative analysis. *Anal. Bioanal. Chem.* **408**, 23–33 (2016).
9. Zhang, J. *et al.* High-throughput salting-out assisted liquid/liquid extraction with acetonitrile for the simultaneous determination of simvastatin and simvastatin acid in human plasma with liquid chromatography. *Anal. Chim. Acta* **661**, 167–172 (2010).
10. Zhang, X. *et al.* SPE-IMS-MS: An automated platform for sub-sixty second surveillance of endogenous metabolites and xenobiotics in biofluids. *Clin. Mass Spectrom.* **2**, 1–10 (2016).
11. van der Laan, T. *et al.* Fast LC-ESI-MS/MS analysis and influence of sampling conditions for gut metabolites in plasma and serum. *Sci. Rep.* **9**, 12370 (2019).
12. Trivedi, D. K., Hollywood, K. A. & Goodacre, R. Metabolomics for the masses: The future of metabolomics in a personalized world. *New Horizons Transl. Med.* **3**, 294–305 (2017).
13. Wang, Z. *et al.* Gut flora metabolism of phosphatidylcholine promotes cardiovascular disease. *Nature* **472**, 57–63 (2011).
14. Mayo Clinic, M. M. L. Rochester 2018 Interpretive Handbook. (2018). doi:10.1016/S1002-0721(13)60014-9
15. Wishart, D. S. *et al.* HMDB 4.0: The human metabolome database for 2018. *Nucleic Acids Res.* **46**, D608–D617 (2018).
16. Matuszewski, B. K., Constanzer, M. L. & Chavez-Eng, C. M. Strategies for the assessment of

matrix effect in quantitative bioanalytical methods based on HPLC-MS/MS. *Anal. Chem.* **75**, 3019–30 (2003).
17. Carducci, C. *et al.* Quantitative determination of guanidinoacetate and creatine in dried blood spot by flow injection analysis-electrospray tandem mass spectrometry. *Clin. Chim. Acta* **364**, 180–187 (2006).
18. Bligh, E.G. and Dyer, W. J. A rapid method of total lipid extraction and purification. *Can. J. Biochem. Physiol.* **37**, (1959).
19. Duisters, K. *et al.* Intersubject and Intrasubject Variability of Potential Plasma and Urine Metabolite and Protein Biomarkers in Healthy Human Volunteers. *Clin. Pharmacol. Ther.* **0**, 1–9 (2019).
20. Thompson, D. K. *et al.* Daily Variation of Serum Acylcarnitines and Amino Acids. *Metabolomics* **8**, 556–565 (2012).
21. Benjamini, Y. & Yekutieli, D. The control of the false discovery rate in multiple testing under dependency. *Ann. Stat.* **29**, 1165–1188 (2001).
22. R Core Team (2017). R: A language and environment for statistical computing. R Foundation for Statistical Computing, Vienna, Austria. Available at: https://www.r-project.org/.
23. Nagu, M., Abdulhadi, A., Huwaiji, A. & Alanazi, N. M. Effect of Elemental Sulfur on Pitting Corrosion of Steels Muthukumar. *Insights Anal. Electrochem.* **4**, 1–7 (2018).
24. Ghosh, C., P. Shinde, C. & S. Chakraborty, B. Ionization Polarity as a Cause of Matrix Effects, its Removal and Estimation in ESI-LC-MS/MS Bio-analysis. *J. Anal. Bioanal. Tech.* **01**, 1–7 (2010).
25. Oldekop, M. L., Rebane, R. & Herodes, K. Dependence of matrix effect on ionization polarity during LC–ESI–MS analysis of derivatized amino acids in some natural samples. *Eur. J. Mass Spectrom.* **23**, 245–253 (2017).
26. Dallmann, R., Viola, A. U., Tarokh, L., Cajochen, C. & Brown, S. A. The human circadian metabolome. *Proc. Natl. Acad. Sci.* **109**, 2625–2629 (2012).
27. Ali, A. H. *et al.* Free fatty acid storage in human visceral and subcutaneous adipose tissue: Role of adipocyte proteins. *Diabetes* **60**, 2300–2307 (2011).
28. Kompare, M. & Rizzo, W. B. Mitochondrial Fatty-Acid Oxidation Disorders. *Semin. Pediatr. Neurol.* **15**, 140–149 (2008).
29. Human Metabolome Database. Available at: http://www.hmdb.ca/.

SUPPLEMENTARY INFORMATION

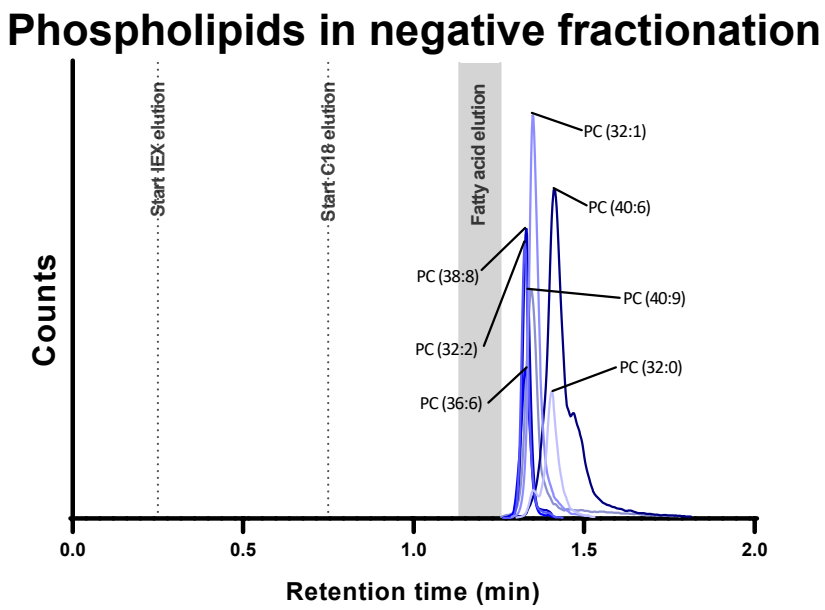

Figure S1. Extracted ion chromatogram of phospholipids in a pooled plasma sample measured by the negative fractionation method and positive MS polarity. The elution window of the fatty acids are indicated by the grey area.

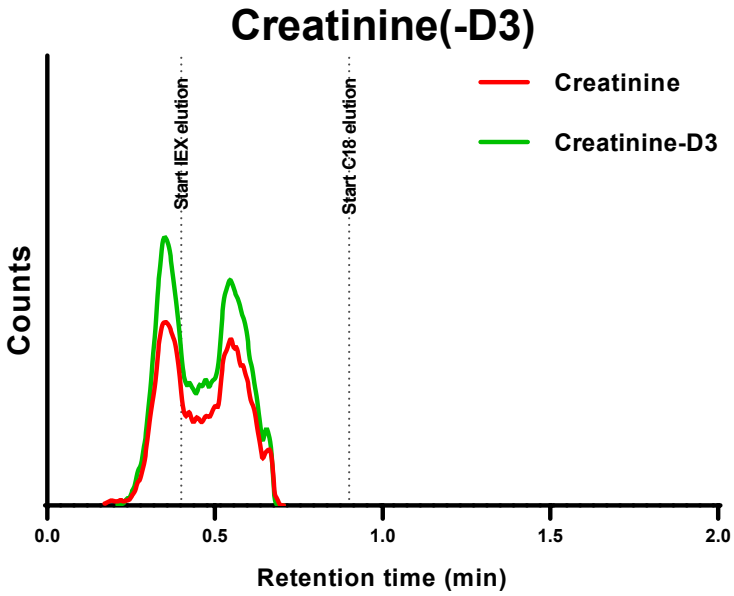

Figure S2. Extracted ion chromatogram of creatinine and creatinine-D3 measured by the fractionation method in a pooled plasma sample in positive mode. The peak shape and retention time are overlapping.

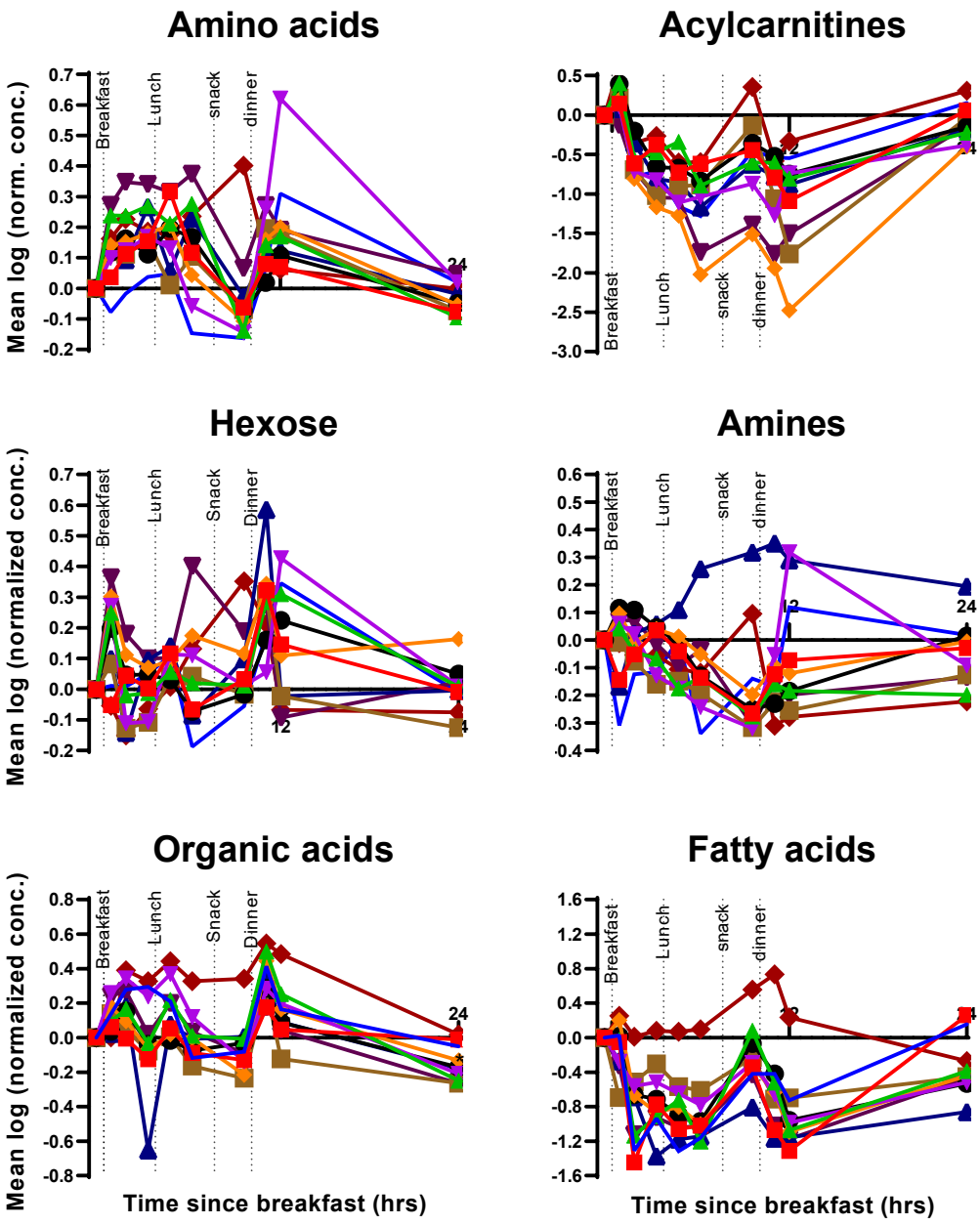

Figure S3. The individual mean natural logarithm of metabolite concentrations over time. Normalization was performed on the first time point. Within each compound class, metabolites were averaged per time point. The 10 volunteers are depicted in different colours. The time frame comprises four standardized feeding times and meals and one night rest. The time is presented with respect to the breakfast time.

Table S1. Calibration standards.

Name	CheBi ID	Standard	Supplier	Solvent	C7 (µM)
1-methylhistidine	70958	1-methylhistidine	HMDB	Water	80
3-methylhistidine	70959	3-methylhistidine	HMDB	Water	40
Alanine	16977	L-alanine	Sigma-Aldrich	Water	1600
Arginine	16467	L-arginine hydrochloride	Sigma-Aldrich	Water	400
Betaine	17750	Betaine hydrochloride	Sigma-Aldrich	Water	300
Carnitine	16347	L-Carnitine hydrochloride	Sigma-Aldrich	Water	200
Citrulline	16349	Citrulline	HMDB	Water	100
Cystine	16283	L-cystine	Fluka	1M Hydrochloric acid	100
Glutamic acid	16015	L-glutamic acid	Sigma-Aldrich	Water	400
Glutamine	18050	L-glutamine	Fluka	Water	2000
Histidine	15971	L-histidine monohydrochloride monohydrate	Fluka	Water	600
Isoleucine	17191	L-Isoleucine	Fluka	Water	200
Leucine	15603	L-Leucine	Fluka	Water	200
Lysine	18019	L-lysine monohydrochloride	Fluka	Water	800
Methionine	16643	L-methionine	Fluka	Water	200
Ornithine	15729	L-Ornithine hydrochloride	Sigma-Aldrich	Water	400
Phenylalanine	17295	L-phenylalanine	Fluka	Water	300
Proline	17203	L-proline	Fluka	Water	800
Serine	17115	L-serine	Fluka	Water	600
Taurine	15891	Taurine	Fluka	Water	400
Threonine	16857	L-threonine	Fluka	Water	600
Tryptophan	16828	L-tryptophan	Sigma-Aldrich	0.5M hydrochloric acid	200
Tyrosine	17895	L-tyrosine	Fluka	1M hydrochloric acid	200
Valine	16414	L-valine	Fkuka	Water	800
TMAO	15724	Trimethylamine-N-oxide dihydrate	Sigma-Aldrich	Water	100
Choline	15354	Choline chloride	Sigma-Aldrich	Water	100
Creatinine	16737	Creatinine	Sigma-Aldrich	Water	400
Urea	16199	Urea	Sigma-Aldrich	Water	10000
Glucose	17634	D-(+)-glucose	Sigma-Aldrich	Water	10000
Guanine	16235	Guanine	HMDB	0.1M sodium hydroxide	8
Hypoxanthine	17368	Hypoxanthine	Sigma-Aldrich	1M sodium hydroxide	200
Uric acid	17775	Uric acid	Sigma-Aldrich	1M sodium hydroxide	2000
Octanoylcarnitine	18102	Octanoyl -L-carnitine HCl	VU medical center	Methanol	1
Decanoylcarnitine	68830	Decanoyl-L-carnitine HCl	VU medical center	Methanol	1
Palmitoylcarnitine	17490	Hexadecanoyl-L-carnitine HCL	VU medical center	Methanol	0,4
Stearoylcarnitine	84644	Octadecanoyl-L-carnitie HCl	VU medical center	Methanol	0,2
Aspartic acid	22660	DL-aspartic acid	Sigma-Aldrich	1M sodium hydroxide	160
Citric acid	30769	Citric acid	Sigma-Aldrich	Water	800
Lactic acid	422	lactic acid lithium salt	Acros organics	Water	3000
Isocitric acid	30887	Isocitric acid	HMDB	Water	40
Pyruvic acid	32816	sodium pyruvate	Sigma-Aldrich	Water	400
Aconitic acid	32805	Cis-aconitic acid	Sigma-Aldrich	Water	225
Alpha-ketoglutaric acid	30915	Alpha-ketoglutaric acid disodium salt hydrate	Fluka	Water	80
2-Hydroxybutyric acid	1148	2-Hydroxybutyric acid sodium salt (97%)	Sigma-Aldrich	Water	400
3-Hydroxybutyric acid	20067	3-hydroxybutyric acid	Sigma-Aldrich	Water	800
Malic acid	6650	DL-Malic acid	Sigma-Aldrich	Water	120
Indoxyl sulfate	43355	indoxyl slufate potassium salt	Sigma-Aldrich	Methanol	20
Alpha-linolenic acid	27432	Alpha-linolenic acid	Cayman chemical	Ethanol	10
Docosahexaenoic acid	28125	Docosahexaenoic acid	Cayman chemical	Ethanol	4
Docosapentaenoic acid	65136	Docosapentaenoic acid	Cayman chemical	Ethanol	2
Linoleic acid	17351	Linoleic acid	Sigma-Aldrich	Methanol	200
Arachidonic acid	15843	Arachidonic acid	Cayman chemical	Ethanol	30
Palmitic acid	15756	Palmitic acid	HMDB	Methanol	200
Oleic acid	16196	Oleic acid	Sigma-Aldrich	Ethanol	200
Stearic acid	28842	Stearic acid	Sigma-Aldrich	Isopropanol	100

Table S2. Internal standards. The C6 values are the concentrations (µM) which were present in the internal standard solution. During sample preparation, the same volume of internal standard solution and plasma is added.

Name	Standard	Supplier	Solvent	C6 (µM)
Phenyl alanine	DL-Phenyl-d5-alanine	CDN isotopes	Water	320
Trimethylamine-N-oxide	Trimethylamine N-oxide-D9	Cambridge Isotope	Water	160
Alanine	DL-ALANINE-2,2,3,3-d3, 99.8% D	CDN isotopes	Water	1600
Choline	Choline-D4 Chloride	CDN Isotopes	Water	60
Carnitine	L-carnitine-d3 HCl (methyl-d3)	CDN Isotopes	Water	180
Creatinine	Creatinine-D3	Cambridge Isotope	Water	360
Valine	L-VALINE (D8)	Cambridge isotopes	Water	800
Leucine	DL-Leucine-D3	CDN Isotopes	1M hydrochloric acid	240
Ornithine	L-Ornithine-D6 hydrochloride	CDN Isotopes	Water	280
Hypoxanthine	Hypoxanthine-D2	CDN Isotopes	1M sodium hydroxide	140
Glutamine	L-GLUTAMINE (2,3,3,4,4-D5)	Cambridge isotopes	Water	2000
Lysine	L-LYSINE 2 HCL (4,4,5,5-D4)	Cambridge isotopes	Water	720
Glutamic acid	L-GLUTAMIC ACID (1,2-13C2)	Cambridge isotopes	1M sodium hydroxide	400
Arginine	L-Arginine-15N2 hydrochloride	Cortecnet	Water	400
Tryptophan	L-TRYPTOPHAN (U-13C11, U15N2)	Cambridge isotopes	Water	200
Glucose	Glucose-13C6	Cortecnet	90% methanol	20000
Octanoylcarnitine	Octanoyl carnitine-D3 HCl	CDN Isotopes	Methanol	0,8
Pyruvic acid	Pyruvic acid-13C3	Omicron Biochemicals	Water	140
Lactic acid	Lactic acid-13C3	Biomedical Isotopes	Water	4000
Malic acid	Malic acid-13C4	Cambridge Isotope	Water	24
Citric acid	Citric acid-D4	Cambridge Isotope	Water	480
Palmitic acid	Palmitic acid-D2	Cambridge Isotope	Ethanol	480
Stearic acid	Stearic acid-D3	Cambridge Isotope	Ethanol	200

Table S3. Solid-phase extraction column information.

Brand	Type	Phase	Functional group	Amount of sorbent (mg)	Particle size (µm)	pH stability	Loading buffer	Elution buffer
Hysphere	SCX	PS-DVB	Sulfonate	13	10	1-14	0.1% formic acid	100 mM ammonium acetate pH 10
Hysphere	SAX	PS-DVB	Quaternary amine	13	10	1-14	5 mM ammonium acetate	1% formic acid
Oasis	WCX	Oasis HLB	Carboxylate	10.4	30	0-14	5 mM ammonium acetate	1% formic acid
Oasis	WAX	Oasis HLB	tertiary/secondary amine	10.4	30	0-14	5 mM ammonium acetate	100 mM ammonium formate pH 10
Sepax	SCX	PS-DVB	Sulfonate	Not disclosed	3	2-12	0.1% formic acid	100 mM ammonium acetate pH 10
Sepax	SAX	PS-DVB	Quaternary amine	Not disclosed	1.7	2-12	5 mM ammonium acetate	1% formic acid
Sepax	WCX	PS-DVB	Carboxylate	Not disclosed	1.7	2-12	5 mM ammonium acetate	1% formic acid
Sepax	WAX	PS-DVB	Tertiary amine	Not disclosed	5	2-12	5 mM ammonium acetate	100 mM ammonium formate pH 10
Zirchrom	SCX	Zirconia dioxide	Ethylenediamine-N,N'-tetramethylphosphonic acid	150	3	1-10	0.1% formic acid	100 mM ammonium acetate pH 10
Zirchrom	SAX	Zirconia dioxide	Polyethyleneimine	150	3	1-12	5 mM ammonium acetate	1% formic acid
Zirchrom	WCX	Zirconia dioxide	Phosphate	150	3	1-10	5 mM ammonium acetate	1% formic acid
Zirchrom	WAX	Zirconia dioxide	Polyethyleneimine	150	3	3-9	5 mM ammonium acetate	100 mM ammonium formate pH 9

Table S4. Fractionation LC and valve parameters for positive mode.

Time (min)	Flow rate (ml/min)	%A	%B	IEX mobile phase	WAX and SCX columns
0.00	0.8	100	0	Out	In
0.40	0.8	100	0	In	In
1.00	0.8	100	0	Out	In
1.01	0.8	0	100	Out	Out
2.10	0.8	0	100	Out	Out
2.11	0.8	100	0	Out	Out
2.35	0.8	100	0	Out	In
3.00	0.8	100	0	Out	In

Table S5. Fractionation LC and valve parameters for negative mode.

Time (min)	Flow rate (mL/min)	%A	%B	IEX mobile phase	WAX column
0.00	0.5	100	0	Out	In
0.25	0.5	100	0	In	In
0.30	0.5	100	0	In	In
0.31	0.8	100	0	In	In
0.75	0.8	100	0	Out	Out
0.76	0.8	20	80	Out	Out
0.95	0.8	15	85	Out	Out
0.96	0.8	0	100	Out	Out
2.00	0.8	0	100	Out	Out
2.01	0.8	100	0	Out	Out
2.25	0.8	100	0	Out	In
3.00	0.8	100	0	Out	In

Table S6. Mass spectrometry parameters.

Platform	Polarity	Gas 1 (psi)	Gas 2 (psi)	Curtain gas (psi)	Temp (°C)	Spray voltage (V)	Declustering Potential (V)	Collision energy (eV)	Mass range (*m/z*)
Fractionation, RP and HILIC	Positive	40	60	40	650	5500	80	5	50-880
	Negative	40	60	40	650	-4500	-60	-5	50-880
FIA	Positive	40	40	30	550	5500	80	5	50-500
	Negative	40	40	30	550	-4500	-80	-5	50-500

Table S7. Overview of the different fractions.

Compounds	pH at loading	Method	Net charge during loading	Fraction	Compound class
Valine/Betaine	2.5	Positive	+/neutral	Flow-through	Amino acids/amines
Leucine/Isoleucine	2.5	Positive	+/neutral	Flow-through	Amino acids
Tryptophan	2.5	Positive	+/neutral	SCX	Amino acids
Trimethylamine-N-oxide	2.5	Positive	Neutral	Flow-through	Amines
Ornithine	2.5	Positive	+/++	SCX	Amino acids
Carnitine	2.5	Positive	+/neutral	Flow-through	Amines
1/3-methylhistidine	2.5	Positive	+/++	SCX	Amino acids
Phenylalanine	2.5	Positive	+/neutral	Flow-through	Amino acids
Serine	2.5	Positive	+/neutral	Flow-through	Amino acids
Citrulline	2.5	Positive	+/neutral	Flow-through	Amino acids
Methionine	2.5	Positive	+/neutral	Flow-through	Amino acids
Arginine	2.5	Positive	+/++	SCX	Amino acids
Alanine	2.5	Positive	+/neutral	Flow-through	Amino acids
Cystine	2.5	Positive	+/++/neutral	SCX	Amino acids
Aspartic acid	2.5	Positive	+/neutral	Flow-through	Amino acids
Glutamic acid	2.5	Positive	+/neutral	Flow-through	Amino acids
Histidine	2.5	Positive	+/++	SCX	Amino acids
Lysine	2.5	Positive	+/++	SCX	Amino acids
Proline	2.5	Positive	+/neutral	Flow-through	Amino acids
Threonine	2.5	Positive	+/neutral	Flow-through	Amino acids
Urea	2.5	Positive	Neutral	Flow-through	Amines
Glutamine	2.5	Positive	+/neutral	Flow-through	Amino acids
Glucose	2.5	Positive	Neutral	Flow-through	Hexose
Tyrosine	2.5	Positive	+/neutral	Flow-through	Amino acids
Choline	2.5	Positive	+	Flow-through	Amines
Hypoxanthine	2.5	Positive	+/neutral	Flow-through	Purines
Guanine	2.5	Positive	+/neutral	Flow-through	Purines
Uric acid	2.5	Positive	Neutral	Flow-through	Amines
Creatinine	2.5	Positive	+	Flow-through/SCX	Amines
Taurine	2.5	Positive	Neutral	Flow-through	Amino acids
Palmitoylcarnitine	2.5	Positive	+/neutral	C18	Acylcarnitines
Stearoylcarnitine	2.5	Positive	+/neutral	C18	Acylcarnitines
Decanoylcarnitine	2.5	Positive	+/neutral	C18	Acylcarnitines
Octanoylcarnitine	2.5	Positive	+/neutral	C18	Acylcarnitines
(Iso)Citric acid	7	Negative	-3	WAX	Organic acids
Malic acid	7	Negative	-2	WAX	Organic acids
Lactic acid	7	Negative	-	Flow-through	Organic acids
Pyruvic acid	7	Negative	-	Flow-through	Organic acids
Aconitic acid	7	Negative	-3	WAX	Organic acids
Alpha-ketoglutaric acid	7	Negative	-2	WAX	Organic acids
2/3-Hydroxybutyric acid	7	Negative	-	Flow-through	Organic acids
Indoxylsulfate	7	Negative	-(sulfate)	WAX	Organic acids
Palmitic acid	7	Negative	-	C18	Fatty acids
Stearic acid	7	Negative	-	C18	Fatty acids
Alpha-linolenic acid	7	Negative	-	C18	Fatty acids
Docosahexaenoic acid	7	Negative	-	C18	Fatty acids
Docosapentaenoic acid	7	Negative	-	C18	Fatty acids
Linoleic acid	7	Negative	-	C18	Fatty acids
Arachidonic acid	7	Negative	-	C18	Fatty acids
Oleic acid	7	Negative	-	C18	Fatty acids

Table S8. Method validation parameters (CO = carryover and ME = matrix effect).

Name	ISTD	Repeatability			Intermediate precision			CO (1st)	CO (2nd)	R^2	ME (%)	LOD (µM)	LLOQ (µM)
		C0 RSD (%)	C2 RSD (%)	C4 RSD (%)	C0 RSD (%)	C2 RSD (%)	C4 RSD (%)						
Val/Bet	Val	1.6	2.0	1.4	3.4	2.8	2.3	0.0	0.0	0.992	71	0.4	1
Leu/Ile	Leu	2.9	1.1	1.7	2.5	3.1	2.9	0.0	0.0	0.993	65	0.5	1
Trp	Tryp	5.8	0.9	2.0	4.7	1.8	2.4	0.0	0.0	0.997	336	0.3	1
TMAO	TMAO	18.1	3.6	1.0	14.8	7.5	3.1	0.0	0.0	0.999	54	0.4	1
Orn	Lys	13.9	3.4	1.4	11.1	6.5	3.8	0.0	0.0	0.994	137	3	10
Carnitine	Car	3.8	0.1	2.0	3.0	1.4	1.7	0.0	0.0	1.000	54	0.01	0.03
1/3-Mhis	Arg	10.5	0.8	1.4	8.8	1.7	2.0	0.0	0.0	0.996			
Phe	Phe	6.6	1.6	3.6	7.2	5.9	4.9	0.0	0.0	0.993	36	1	4
Ser	Val	6.3	2.4	1.9	4.9	4.6	4.2	0.0	0.0	0.994			
Cit	Val	3.9	2.1	2.6	6.0	4.7	5.8	0.0	0.0	0.997			
Met	Val	5.4	1.8	1.6	5.1	3.8	3.5	5.3	1.5	0.999			
Arg	Arg	3.3	1.2	0.8	3.6	1.8	2.3	2.0	0.0	0.999	89	0.2	0.5
Ala	Glu	4.7	1.4	3.8	5.2	2.3	3.8	0.0	0.0	0.997	68	8	27
Cys-Cys	Lys	6.0	2.2	3.7	7.9	3.3	5.0	0.0	0.0	0.991			
Asp	Val	4.8	3.7	4.3	5.9	6.3	4.2	0.0	0.0	0.995			
Glu	Leu	3.2	0.7	1.4	3.2	3.5	2.4	0.0	0.0	0.996	91	0.9	1
His	Arg	12.1	1.6	0.9	10.0	4.6	2.9	0.5	0.1	0.995			
Lys	Lys	4.3	2.7	3.3	3.6	3.0	3.1	0.0	0.0	0.995	130	1	4
Pro	Val	2.3	1.9	2.4	1.8	2.1	1.6	0.0	0.0	0.998			
Thr	glu	5.7	1.8	3.2	4.2	4.7	2.4	0.0	0.0	0.995			
Urea	Phe	4.2	3.9	3.4	4.7	3.1	2.4	0.0	0.0	0.993			
Gln	glu	3.6	0.7	2.0	2.7	1.9	1.8	0.0	0.0	0.999	69	1	4
Glucose	Glucose	7.2	1.2	7.9	5.3	2.7	5.1	0.0	0.0	0.998	77	3	10
Tyr	Glu	2.2	6.4	3.7	4.4	7.6	4.1	0.0	0.0	0.999			
Choline	Choline	3.4	1.4	1.2	2.7	1.5	1.6	0.0	0.0	0.999	81	0.04	0.1
Hyp	Phe	6.6	4.2	1.2	12.1	4.9	2.7	0.0	0.0	0.998			
Gua	Leu	18.9	8.2	6.5	15.4	8.8	6.7	0.0	0.0	0.991			
Urate	Glu	1.6	2.2	1.3	2.3	3.7	4.3	0.0	0.0	0.991			
Creat	Creat	4.2	0.4	1.5	3.4	1.3	1.3	0.0	0.0	0.999	49	0.09	0.3
Tau	Glu	3.2	2.1	2.6	3.7	4.4	4.4	0.0	0.0	0.997			
C16 carnitine	C8 carnitine	3.8	4.0	1.4	5.5	9.0	10.0	1.8	0.0	0.982			
C18 carnitine	C8 carnitine	11.6	6.0	3.3	11.2	11.7	6.9	0.0	0.0	0.987			
C10 carnitine	C8 carnitine	4.1	1.4	5.4	9.1	6.0	8.6	2.4	1.3	0.990			
C8 carnitine	C8 carnitine	4.6	3.1	5.0	5.8	3.8	4.1	0.0	0.0	0.994	98	0.002	0.003
Citrate	Citrate	1.5	1.3	3.5	2.0	1.8	3.3	0.3	0.2	0.999	562	0.7	1
Malate	Malate	10.6	3.2	0.6	14.7	5.1	3.9	0.4	0.0	0.993	75	0.4	0.9
Lactate	Lactate	1.5	0.7	4.1	1.9	3.0	2.7	0.0	0.0	0.991	34	5	13
Pyruvate	Lactate	4.0	4.8	2.9	4.9	4.9	5.0	0.0	0.0	0.993	41	9	19
Aconate	Citrate	5.8	1.9	3.2	8.5	4.7	3.6	0.9	0.0	0.998			
α-keto-glutarate	Citrate	8.5	7.3	4.1	11.4	6.8	6.6	2.0	0.1	0.996			
2/3-hydroxy-butyrate	Lactate	8.3	0.6	0.7	7.0	4.0	3.2	0.0	0.0	0.999			
Indoxyl-sulfate	Citrate	3.1	3.7	7.3	9.6	6.7	8.0	0.0	0.0	0.995			
FA(16:0)	FA(16:0)	8.9	10.1	10.9	13.5	8.6	11.0	0.8	0.0	0.996	94	0.6	0.7
FA(18:0)	FA(16:0)	9.2	6.6	5.0	14.4	8.4	9.7	0.0	0.0	0.996	98	0.2	0.6
FA(18:3)	FA(16:0)	3.6	3.7	0.9	13.6	14.3	6.9	1.9	0.8	0.996			
FA(22:6)	FA(16:0)	7.6	2.3	0.3	6.9	4.5	6.2	0.4	0.0	0.998			
FA(22:5)	FA(18:0)	6.3	12.6	2.5	7.9	10.7	6.8	1.6	0.3	0.974			
FA(18:2)	FA(18:0)	5.0	3.3	2.2	11.6	5.6	2.7	1.2	0.3	0.998			
FA(20:4)	FA(18:0)	4.9	3.0	1.9	7.9	3.8	4.5	2.0	0.6	0.998			
FA(18:1)	FA(18:0)	3.7	6.0	2.1	4.7	6.4	5.2	0.9	0.1	0.996	562		

Table S9. The matrix effect and fraction of 22 internal standards in fractionation, liquid-liquid extraction coupled to flow injection analysis (LLE-FIA) and flow injection analysis (FIA). An ion suppression of 0% indicates a compound that is either enhanced or not suppressed. An ion suppression of 100% means that the compound is not detected.

Compounds	Fractionation		LLE-FIA		FIA
	Matrix effect (%)	Fraction	Matrix effect (%)	fraction	Matrix effect (%)
Valine-d8	71	Flow-through	5	Polar	1
Leucine-d3	65	Flow-through	4	Polar	0
Tryptophan-13C11, 15N2	336	SCX	4	Polar	0
TMAO-d9	54	Flow-through	9	Polar	4
Ornithine d6	137	SCX	2	Polar	0
Carnitine-d3	54	Flow-through	14	Polar	6
Phenylalanine-d5	36	Flow-through	4	Polar	1
Arginine-15N2	89	SCX	7	Polar	3
Alanine-d3	68	Flow-through	0	Polar	0
Glutamic acid-13C2	91	Flow-through	0	Polar	0
Lysine-d4	130	SCX	5	Polar	2
Glutamine-d5	69	Flow-through	1	Polar	0
Glucose-13C6	77	Flow-through	25	Polar	17
Choline-d4	81	Flow-through/SCX	24	Polar	14
Creatinine-d3	49	Flow-through	20	Polar	6
Octanoyl carnitine-d3	98	C18	32	Apolar	8
Citric acid-D4	562	WAX	86	Polar	677
Malic acid-13C4	75	WAX	19	Polar	24
Lactic acid-13C3	34	Flow-through	14	Polar	14
Pyruvic acid-13C3	41	Flow-through	11	Polar	15
Palmitic acid-D2	94	C18	76	Apolar	12
Stearic-D3	98	C18	70	Apolar	10

Table S10. The LLOQ of literature LC-MS methods. The LLOQ determination, MS mode, derivatization, analysis time and reference are also indicated in the table.

	LLOQ (µM)	LLOQ determination	MS mode	Derivatization	Analysis time (min)	Reference
Valine	10	Unknown	Tandem	Yes	7	Trabado *et al.*[1]
Leucine	10	Unknown	Tandem	Yes	7	Trabado *et al.*[1]
Tryptophan	5	Unknown	Tandem	Yes	7	Trabado *et al.*[1]
TMAO	0.1	S/N	Tandem	No	10	Liu *et al.*[2]
Ornitine	5	Unknown	Tandem	Yes	7	Trabado *et al.*[1]
Carnitine	0.06	S/N	Tandem	No	10	Liu *et al.*[2]
Phenyl alalnine	5	Unknown	Tandem	Yes	7	Trabado *et al.*[1]
Arginine	5	Unknown	Tandem	Yes	7	Trabado *et al.*[1]
Alanine	20	Unknown	Tandem	Yes	7	Trabado *et al.*[1]
Glutamic acid	5	Unknown	Tandem	Yes	7	Trabado *et al.*[1]
Lysine	10	Unknown	Tandem	Yes	7	Trabado *et al.*[1]
Glutamine	20	Unknown	Tandem	Yes	7	Trabado *et al.*[1]
Glucose	11	S/N	Tandem	No	4	Matsunami *et al.*[3]
Choline	0.1	S/N	Tandem	No	10	Liu *et al.*[2]
Creatinine	10	Unknown	Tandem	Yes	7	Trabado *et al.*[1]
C8 carnitine	0.006	S/N	Tandem	Yes	22	Giesbertz *et al.*[4]
Citrate	0.2	S/N	Tandem	No	Unknown	Kadhi *et al.*[5]
Malate	0.2	S/N	Tandem	No	Unknown	Kadhi *et al.*[5]
Lactate	3	S/N	Tandem	No	Unknown	Kadhi *et al.*[5]
Pyruvate	1	Unknown	Tandem	No	3.5	Chuang *et al.*[6]
FA(16:0)	0.8	Calibration curve	High-resolution	No	15	Takahashi *et al.*[7]
FA(18:0)	0.07	calibration curve	High-resolution	No	15	Takahashi *et al.*[7]

References Table S10

1. Trabado, S. *et al.* The human plasma-metabolome: Reference values in 800 French healthy volunteers; Impact of cholesterol, gender and age. *PLoS One* **12**, 1–17 (2017).

2. Liu, J. *et al.* Simultaneous targeted analysis of trimethylamine-N-oxide, choline, betaine, and carnitine by high performance liquid chromatography tandem mass spectrometry. *J. Chromatogr. B Anal. Technol. Biomed. Life Sci.* **1035**, 42–48 (2016).

3. Matsunami, R. K., Angelides, K. & Engler, D. A. Development and validation of a rapid 13C6-Glucose Isotope Dilution UPLC-MRM Mass Spectrometry Method for Use in determining system accuracy and performance of blood glucose monitoring devices. *J. Diabetes Sci. Technol.* **9**, 1051–1060 (2015).

4. Giesbertz, P., Ecker, J., Haag, A., Spanier, B. & Daniel, H. An LC-MS/MS method to quantify acylcarnitine species including isomeric and odd-numbered forms in plasma and tissues. *J. Lipid Res.* **56**, 2029–2039 (2015).

5. Al Kadhi, O., Melchini, A., Mithen, R. & Saha, S. Development of a LC-MS/MS Method for the Simultaneous Detection of Tricarboxylic Acid Cycle Intermediates in a Range of Biological Matrices. *J. Anal. Methods Chem.* **2017**, 1–12 (2017).

6. Chuang, C. K. *et al.* A method for lactate and pyruvate determination in filter-paper dried blood spots. *J. Chromatogr. A* **1216**, 8947–8952 (2009).

7. TAKAHASHI, H. *et al.* Long-Chain Free Fatty Acid Profiling Analysis by Liquid Chromatography–Mass Spectrometry in Mouse Treated with Peroxisome Proliferator-Activated Receptor α Agonist. *Biosci. Biotechnol. Biochem.* **77**, 2288–2293 (2013).

Table S11a. The reversed phase (RP) gradient performed on an UPLC HSS T3 (1.7 µm, 2.1 x 100 mm). Mobile phase A and B consisted of 0.1% formic acid in water and acetonitrile, respectively. The column oven was set at 30 °C. The sample preparation, injection volume and MS parameters were similar to the fractionation method.

Time (min)	Mobile phase B (%)	Flow rate (mL/min)
0.0	0	0.4
7.0	15	0.4
10	55	0.4
10.5	100	0.4
12.5	100	0.4
12.6	0	0.4
15.0	0	0.4

Table S11b. The hydrophilic interaction liquid chromatography (HILIC) gradient performed on a Sequant ZIC-HILIC (3 µm, 2.1 x 100 mm). Mobile phase A consisted of 10 mM ammonium formate and 0.075% formic acid in 90/10 (v/v) acetonitrile/water and mobile phase B of 10 mM ammonium formate and 0.075% formic acid in 10/90 (v/v) acetonitrile/water. The column oven was set at 30 °C. The sample preparation, injection volume and MS parameters were similar to the fractionation method.

Time (min)	Mobile phase B (%)	Flow rate (mL/min)
0.0	0	0.5
1.2	0	0.5
9.16	75	0.5
14.0	75	0.5
14.2	0	0.5
18.0	0	0.5

Table S11C. The number of detectable features in the fractionation, RP and HILIC method as determined by the 'Non-targeted Peaks' function in Analytics of Sciex OS 1.6. The minimum retention time was determined by the dead volume of the platform and the maximum retention time was determined by the start of the column equilibration. The peak detection sensitivity was set at exhaustive, the Area Ratio Threshold (Unknown/Control) was set at 0 and the 'Group peaks by adduct or charge' function was checked. The number of features was corrected for the presence of multiple adducts. Feature m/z values were rounded to two decimal points. Features that were identified in both positive and negative mode were indicated as one feature.

Platform	Unique retention time and m/z features	Unique m/z features
Fractionation	2342	2113
RP	3517	2478
HILIC	3534	2326

Table S12. P-values and FDR adjusted p-values of several compound classes on different time points in comparison to baseline levels.

Compound class	Time after breakfast (hours)	P-value	FDR adjusted p-value
Amino acids	0.5	0.006	0.063
	1.5	0.004	0.046
	3	0.002	0.032
	4.5	0.002	0.032
	6	0.037	0.296
	9.5	0.16	0.942
	11	0.002	0.032
	12	0.002	0.032
	24	0.131	0.829
Amines	0.5	0.846	1
	1.5	0.557	1
	3	0.232	1
	4.5	0.105	0.686
	6	0.064	0.498
	9.5	0.084	0.576
	11	0.084	0.576
	12	0.557	1
	24	0.16	0.942
Acylcarnitines	0.5	0.014	0.13
	1.5	0.002	0.032
	3	0.002	0.032
	4.5	0.002	0.032
	6	0.002	0.032
	9.5	0.006	0.063
	11	0.002	0.032
	12	0.002	0.032
	24	0.232	1
Hexose	0.5	0.02	0.166
	1.5	0.77	1
	3	0.922	1
	4.5	0.002	0.032
	6	0.557	1
	9.5	0.16	0.942
	11	0.002	0.032
	12	0.084	0.576
	24	1	1
Organic acids	0.5	0.002	0.034
	1.5	0.004	0.046
	3	0.846	1
	4.5	0.006	0.058
	6	0.846	1
	9.5	0.105	0.686
	11	0.002	0.034
	12	0.02	0.166
	24	0.006	0.058
Fatty acids	0.5	0.193	1
	1.5	0.004	0.046
	3	0.004	0.046
	4.5	0.004	0.046
	6	0.004	0.046
	9.5	0.105	0.686
	11	0.037	0.296
	12	0.004	0.046
	24	0.01	0.097